This is a preprint, the final version is subject to change, of the American Mineralogist (MSA)
Cite as Authors (Year) Title. American Mineralogist, in press.
DOI: https://doi.org/10.2138/am-2018-6448

***Revision 1***

# Electrical Cell Assembly

# for Reproducible Conductivity Experiments in the Multi-Anvil

Anne Pommier[1]* and Kurt D. Leinenweber[2]

[1] UCSD-SIO, Institute of Geophysics and Planetary Physics, La Jolla, CA, USA

[2] ASU, School of Molecular Sciences, Tempe, AZ, 85287-1604, USA

* Corresponding author. Email: pommier@ucsd.edu

**Abstract**

Electrical conductivity experiments under pressure and temperature conditions relevant to planetary interiors are a powerful tool to probe the transport properties of Earth and planetary materials as well as to interpret field-based electrical data. In order to promote repeatability and reproducibility of electrical experiments among multi-anvil facilities that use this technique, we designed and developed an electrical conductivity cell for multi-anvil experiments based on the 14/8 assembly that was developed to allow access to high temperatures. Here we present the details of design and parts developed for this cell that is available via the Consortium for Material Properties Research in Earth Sciences (COMPRES). The electrical cell has been tested up to 10 GPa and about 2,000°C on different materials (silicates and metals, both in the solid and liquid state).

**INTRODUCTION**

Laboratory measurements of the electrical properties of Earth's and planetary materials benefitted directly from the knowledge gained in material science and, in particular, electrochemical studies on aqueous solutions (e.g., Noyes et al., 1907; Fogo et al., 1954; Quist and Marshall, 1968) and on solids (e.g., Bauerle, 1969) that have been conducted since the beginning of the 20$^{th}$ century. Among the different setups developed, a common challenge consisted of avoiding polarization of the electrodes and in the sample, which can be accomplished by applying a small alternating current through the cell. Because semi-conductor materials present a frequency dependent electrical behavior, efforts were also made to conduct electrical measurements over a scan in frequency (e.g., Koops, 1951). The abundance of semi-conductor silicates in the crust and mantle of the Earth (and other terrestrial bodies) (e.g., Knight, 1984; Sato et al., 1986) motivated geoscience studies to develop setups allowing measurements of the dispersion in frequency of rock samples under ever-increasing pressure and temperature. Among the different methods to visualize the electrical response of a semiconductor, the graphic representation of the sample's complex impedance (e.g., Roberts and Tyburczy, 1991; Huebner and Dillenburg, 1995) has become the most commonly used and experimental petrology facilities show a widespread usage of the impedance spectroscopy technique. In contrast, electrical studies of conductors (such as metallic core analogues) under pressure and temperature do not require measurements to be conducted over a range in frequency (e.g., Secco and Schloessin, 1989; Deng et al., 2013; Silber et al., 2017); conductors present a very low capacitance and the frequency where induction equals zero is temperature-independent (Constable, 2015).

Different technical challenges arise from *in situ* and real-time electrical measurements under pressure and temperature, such as minimizing noise from the furnace on the electrical data and avoiding the breaking of the electrodes during compression. Among the different pressure device used in experimental geosciences, the multi-anvil apparatus is a relevant tool to conduct electrical investigations. First, by covering a broader pressure and temperature range than piston-cylinders and internally or externally-heated pressure vessels, it reproduces the pressure conditions of the Earth's crust and upper mantle as well as the entire interior of several small terrestrial bodies (such as Mars, Mercury, Ganymede, the Moon). Furthermore, recent development of high pressure techniques using a Kawai-type multi-anvil press suggests that the maximum attainable pressure can reach up to 60 and 120 GPa using WC anvil and sintered diamond anvil, respectively. Second, multi-anvil investigations can be conducted on larger sample volumes than in very high-pressure devices such as diamond-anvil cells (DAC) and provide better constraints on temperature than DAC experiments.

The success of high-pressure and high-temperature electrical experiments to address geoscience questions depends on the quality and reproducibility of the measurements, as well as precise inter-laboratory comparisons. COMPRES, the Consortium for Material Properties Research in Earth Sciences, supported this study that consists of designing a 14/8 electrical assembly for the multi-anvil apparatus that can be used at pressure (up to about 10 GPa) and temperature (up to about 2,000°C) conditions relevant to terrestrial bodies, including the Earth. Here we present the development and testing of this electrical cell, which is adapted from the COMPRES cell assemblies (Leinenweber et al., 2012), and document the materials used as well as the calibration. This cell is available through COMPRES and interested experimentalists should be able to reproduce and adapt the cell with the designs and descriptions provided in this paper.

## DESIGN OF THE ELECTRICAL CELL ASSEMBLY

### Assembly parts and sources

The electrical cell is adapted from the 14/8 COMPRES high-temperature equatorial assembly and uses the same suppliers (Leinenweber et al., 2012). These suppliers have shown to be able to provide all the required parts in sufficient quantities to support a large usage in numerous multi-anvil facilities. A straight-heater rhenium assembly was developed to allow access to higher temperatures (where graphite breaks down) in the range of 8-14 GPa. The octahedron from the Bayreuth 14/8 assembly (with a 5.6 mm hole) was used, a straight full-length zirconia sleeve fits inside the octahedron, and a Re heater with a one-layer 125-micron thick foil is employed inside the zirconia sleeve. MgO rods and tubes with 3.5 mm outer diameter are used inside the furnace, and a maximum sample volume of 3 mm outer diameter and 3 mm length can be achieved in this assembly.

For electrical conductivity measurements, the sample length is reduced and all parts are made from porous MgO, with no alumina included. The sources and dimensions of materials are listed in **Table 1** and a sketch of the electrical assembly is presented in **Figure 1**. Two types of electrical experiments can be performed with the electrical cell assembly: 2-electrode (**Figure 1a**) or 4-electrode (**Figure 1b**) experiments. Three W-Re wires are present in the 2-electrode cell, with one wire serving as both a thermocouple wire and an electrode. The 4-electrode cell contains four W-Re wires, serving either as four electrodes or as two thermocouples. As discussed below, in the case of 2-electrode experiments, the electrical contribution of the electrodes involved in the bulk measurements resistance typically corresponds to a few ohms and needs to be removed from the bulk resistance in order to obtain the sample (Pommier et al., 2010). If this resistance value is negligible compared to the much higher electrical resistance (lower electrical conductivity) of silicate minerals (e.g., Tyburczy and Fisler, 1995), it can represent a significant amount of the bulk electrical response and even hide the sample's response in case the resistance of the sample is smaller than that of the electrodes, which happens for samples containing silicate and carbonate liquids and metals. Getting rid of most of the electrode contribution can be achieved with the 4-electrode setup, where the configuration prevents the applied current from being delivered in the loop of measurement formed by the electrodes. With this setup, four thermocouple wires are connected two-by-two on the metal disk, each of them corresponding to either a voltage probe or a current probe (**Figure 1b**). In this configuration, the measured bulk resistance only needs to be corrected for the metal disks, as the wires are not part of the electrical measurement like they are with the 2-electrode setup. For both 2-electrode and 4-electrode experiments, the sample is in direct contact with the two metal disks and the MgO middle sleeve that contains the sample. The purpose of the metal disks is two-fold: 1) to prevent direct contact between the sample and thermocouple wire, and 2) by covering the sample's extremities, to promote the distribution of current through the entire volume of the sample (e.g., Kennedy, 1960). Note that in semiconductors, current distribution also depends on the sample length:electrode diameter ratio and is optimized when the ratio is close to 1 (Kennedy, 1960).

The chemical interactions between the sample and these parts are discussed below. No capsule contains the sample and the absence of capsule is motivated by the requirement of having the electrode disks in direct contact with the sample and the W-Re leads. We observe that the effect of pressure helps contain a partially molten sample until high melt fractions (Pommier et al., 2015a, 2015b). However, depending on the sample's texture and melt chemistry, the mobility of the liquid phase at high temperature may be high enough to escape along the inner wall of the MgO sleeve and eventually leave the cell (e.g., Yoshino et al., 2003; Zhang and Pommier, 2017). One way to circumvent this issue is to minimize the melt fraction and the time spent at temperature above the melting point of the phase that melts first. At high temperatures (> melting point), there is a balance to find between reaching electrical equilibrium (which does not guarantee chemical equilibrium) and minimizing melt escape.

Crushable MgO sleeves and MgO 4-bore beads are preferred to alumina parts due to the low hardness of crushable MgO compared to fully dense alumina. Tests on partially molten samples using a cell containing 4-bore alumina showed that sample deformation is higher than with 4-bore MgO. This implies that the geometric factor of the sample, corresponding to the electrode area/sample length, is affected during the experiment with alumina. Since the electrical conductivity $\sigma$ of the sample directly depends on the geometric factor G with the relationship

$$\sigma = 1/(R \times G) \quad (1)$$

with R being the electrical resistance, a higher uncertainty on the electrical measurements occurs when the 4-bore beads that host the metallic wires are made of alumina. All MgO parts used in this assembly are fired at 1400°C to fully remove any carbon contaminants, and also to increase the crystallinity and reduce the possibility of surface hydration of the MgO during exposure to air.

**Other cell components**

Similarly to the 14/8 COMPRES assemblies (Leinenweber et al., 2012), the electrical cell assembly is used with Toshiba Tungaloy carbide cubes for the 14/8 size, and can also be used with Rockland Research carbide cubes. The plastic pads at the interface between the tungsten-carbide cubes and the anvils are made of fiberglass-impregnated phenolic resin (called “G-10”). Twelve pyrophyllite gaskets (6 short and 6 long) have the same dimensions and source as the ones used in Leinenweber et al. (2012) for the 14/8 assemblies. Depending on the type of electrical experiment (2 or 4 W-Re wires, **Figure 1**), 3 or 4 grooves need to be made on the side of gaskets, using either a thin diamond file or a hand drill with appropriate drill bit. Four pieces of 3-ply paper are used on the four tungsten-carbide cubes as backing of the pyrophyllite gaskets. Their dimensions and source are similar to the other 14/8 COMPRES assemblies. We recommend to wrap the other four tungsten-carbide cubes with 5 mil Teflon tape in order to minimize risks of short-circuit between the electrode wires and the tungsten-carbide cubes.

**Development of the electrical cell: modifications from the standard 14/8 assembly**

The presence of 3 or 4 W-Re wires (for 2- and 4-electrode experiments, respectively) required the development of a 4-notch octahedron. The design of the pressure medium is illustrated in **Figure 2a**. As in the COMPRES 14/8 equatorial assemblies, the octahedron is an injection-molded ceramic essentially made of MgO and alumina that turn into spinel and periclase after firing at high temperature (1535°C) (Leinenweber et al., 2012). In the case of 2-electrode experiments, one of the four notches is left unused, as this configuration involves only 3 wires (**Figure 1a**). We recommend to simply fill this notch with the electrically resistant cement that is applied on both ends of the cell assembly.

The laser-cut rhenium furnace is also re-designed to contain four grooves for this assembly. The four notches are aligned with the four grooves in the octahedron. The geometry of the rhenium foil is presented in **Figure 2b**. One improvement of the furnace from the COMPRES 14/8 equatorial assemblies is the increase in the groove width (1.2 mm), improving the isolation between the furnace and the W-Re wires, hence minimizing the risk for short-circuit. Again, one notch in the rhenium foil will be left unused when preparing a 2-electrode cell assembly.

## TESTING AND CALIBRATION OF THE ELECTRICAL CELL

This cell has been tested up to 2000°C (Pommier et al., 2015a) and 10 GPa (Pal et al., in prep.). It should work up to 14 GPa, like the standard 14/8 cell it is derived from.

### Effect of the furnace on electrical measurements

#### *Furnace chemistry and electrical measurements*

Two types of furnaces were tested, rhenium and graphite. In order to evaluate the effect of furnace chemistry, and in particular, the redox environment it may contribute to impose on the sample's response, electrical measurements were conducted on the same sample (polycrystalline San Carlos olivine) at similar pressure and temperature conditions. Olivine conductivity being sensitive to oxygen fugacity (e.g., Schock et al., 1989), it is a relevant material to use to probe the effect of the furnace type on the electrical measurements. As illustrated in **Figure 3**, sample conductivity is not affected by furnace type (that is graphite versus rhenium) at the timescale of electrical experiments (duration of about two hours each), though these two furnaces would produce relatively different redox conditions, i.e., reducing and oxidizing environment, respectively. This observed insignificant effect of heater chemistry on oxygen fugacity is also due to the fact that the experiment is not buffered (for instance, at the Re-$ReO_2$ oxygen buffer) since the components of the cell and the sample do not bring both sides of the redox buffer equation.

*Noise from the furnace on electrical measurements*

The electrical cell does not contain a shielding such as a Faraday cage. A Faraday cage is needed when electromagnetic radiation reaches the sample while electrical measurements are being performed, and the presence of a thermal insulator (in our case, the MgO sleeves) will not stop the radiation. This radiation strongly depends on the level of electromagnetic noise in the lab and can be minimized or erased with shielding. Having the multi-anvil press shielded represents an efficient Faraday cage, and the cell was tested both at ASU and UCSD-SIO, where the presses are shielded to the ground with no major source of radiation around. In case the cell is used in a press that is not shielded or is located in an environment with nearby sources of electromagnetic noise, interferences might affect the electrical measurements and one solution is to wrap the sample with a metal foil (e.g., Xu et al., 1998; Kavner and Walker, 2006). In this case, it is critical to ensure that the shielding foil and the electrodes are not in contact, to avoid a short-circuit.

Interferences between furnace and electrical measurements would be directly detected with the impedance technique, as any coupling between the sample and the furnace would affect the shape of the impedance response and increase noise on the collected data over at least part of the frequency range. As illustrated in **Figure 4**, the electrical cell provides high-quality spectra over wide frequency ranges.

**Interactions between the sample and cell parts**

Experiments on silicates and on metals suggest that at the timescale of electrical experiments (typically a few hours), the MgO middle sleeve does not significantly react with the sample (Pommier et al., 2015a,b; Zhang and Pommier, 2017). Experiments on Fe-bearing materials (polycrystalline San Carlos olivine and iron alloys) at temperature up to 1800°C present the development of a thin (<100 microns) ferropericlase layer at the sample-MgO sleeve interface (**Figure 5**). The contribution of this thin (Mg,Fe)O layer to the bulk electrical response can be estimated using the conductivity of ferropericlase. Since the sample and ferropericlase arrangement corresponds to a parallel model, the bulk electrical conductivity (effective resistance) of the circuit can be written as follow (e.g., Glover et al., 2000)

$$\frac{1}{R_{bulk}} = \frac{X_{per}}{R_{per}} + \frac{1-X_{per}}{R_{sample}} \quad (2)$$

where $R_{bulk}$ is the bulk electrical resistance (ohm), $X_{per}$ the volume fraction of periclase, $R_{per}$ the resistance of periclase (ohm) from Yoshino et al. (2011) with a $X_{Fe}$ of 0.2-0.3, and $R_{sample}$ the resistance of the sample (ohm). The electrical conductivity is calculated using Eq. 1. Application of Eqs. 1 and 2 to the experiment on San Carlos olivine (sample shown in **Figure 5b**), considering a volume fraction of periclase of about 0.2 and the estimated sample conductivity over the T range 700-1864°C (we do not expect periclase formation to occur at lower temperature), suggests that the sample conductivity represents >99.6 % of the measured bulk conductivity, highlighting the negligible contribution of periclase on the bulk electrical response.

The electrical cell has been tested with two types of electrodes, molybdenum and iron. These materials have been selected mostly because of their high melting point (1538°C and 2623°C at 1 bar for Fe and Mo, respectively) that allows collecting electrical data over a wide temperature range. Another important criterion is the minimization of chemical interactions with the sample bracketed by the metal disks. Experiments on silicates up to 6 GPa suggested that chemical contamination from the electrodes is insignificant up to very high temperature when a high melt fraction is present in the sample (> about 1800°C for partially molten olivine samples and MORB+olivine samples; Pommier et al., 2015a, 2015b). Electrical experiments up to 6 GPa on olivine-iron alloys showed that Mo contamination of liquid metallic alloys is significant if the sample is kept for a few minutes above the melting temperature of the iron alloy (Yoshino et al., 2004; Zhang and Pommier, 2017). The samples being in direct contact with molybdenum or iron, it is possible that the metal disks get lightly oxidized during the experiments when the sample contains oxygen. However, it is unlikely to be a significant oxidation due to the limited time that the sample spends at high temperature. In any case, it is necessary to analyze the chemistry of retrieved samples to estimate the level of contamination from the electrodes using EDS SEM or electron microprobe analyses.

Electrode deformation (as observed in **Figure 5b**) can occur and may be favored at high pressure and high temperature. It may also occur during decompression, after quenching the experiment. If necessary, electrode disks can be doubled on each side to minimize deformation (a blank experiment will be required to estimate the bulk electrodes contribution). Electrode deformation should be accounted for as part of the calculation of uncertainty on conductivity, as it affects the sample thickness that is part of the geometric factor G (Equation 1). The change in sample length with P and T introduces a systematic bias because the final length of the sample is usually a minimum length for the entire experiment. Based on experience with *in-situ* radiography, the final length is reached once the sample reaches the temperature condition where it is soft enough to lose all its porosity (usually around 800 °C for silicates). The sample length then varies primarily with thermal expansion, elastic response to pressure changes, phase transformations, and ductile flow. Elastic considerations mean that the sample length is less at high pressure, while ductile flow means the sample length could have been greater. Because we cannot estimate these effects well without having an *in-situ* capability, we consider the length after the experiment to be the preferred representation of sample length during the measurement.

**Contribution of the electrodes to the measured electrical resistance**

In the case of 2-electrode experiments, it is critical to evaluate the electrode contribution to the measured (bulk) resistance in order to have an accurate estimate of the sample's electrical resistance (e.g., Pommier et al., 2010). The setup we used to test and calibrate the electrical cell considers electrodes made of four components: two metal disks (each being 0.2 mm thick and 2 mm in diameter), two W-Re thermocouple wires protected by a Teflon sleeve (each being about 10 cm long and 178 micron in diameter, which is thin enough for the anvil gap (at least 1 mm) up to the highest pressure), two W-Re metallic wires that connect the wires inside the press to the outside (each being about 30 cm long and 0.5 mm in diameter), and four 50 cm-long BNC cables that are plugged to the Solartron impedance spectrometer. Minimizing the length of cables and wires between the spectrometer and the press minimizes the electrode resistance. We performed a blank electrical experiment at 3 GPa and over a wide temperature range (up to 1450°C) at UCSD-SIO. No sample was placed in the cell, i.e. the metal disks were in direct contact, and measurements were taken during heating and cooling cycles. As highlighted in **Figure 6**, the results suggest that 1) the electrode resistance is about 7.5 Ohm, 2) this value is not temperature-dependent, and 3) this value does not change significantly at the timescale of the electrical experiments (total duration of about 2 hours). A similar value was obtained with the two-electrode setup at ASU for a blank experiment conducted at 4 GPa and temperature up to 1900°C and using the same electrical cell (Pommier et al., 2015a).

In 4-electrode experiments, only the Mo or Fe disks are added to the bulk measurements. Based on the geometry of the disks and on the conductivity of the metal, their contribution to the electrical measurement can be easily estimated but it can also be measured as part of a blank experiment. From 700 to 1500°C, the calculated resistance of Mo disks represents 4.3-$8.3 \times 10^{-5}$ ohm and the one of Fe disks 2-$2.7 \times 10^{-4}$ ohm. These resistance values need to be deduced from the bulk resistance, as sample and disks form a series circuit.

**Thermal gradient**

Electrical conductivity of Earth's and planetary materials being very sensitive to temperature, it is important to minimize temperature variations across the sample. The thermal gradient in the electrical cell was estimated in different ways. Because 4-electrode experiments contain two thermocouples (**Figure 1b**), it provides a temperature reading on both sides of the sample during the electrical experiment. If this technique does not measure directly the thermal gradient across the sample, it allows checking the temperature at the extremities of the sample and verify whether or not the sample is centered in the hotspot zone of the assembly. The absence of a thermal gradient across the sample can be evaluated after the electrical experiment by checking the chemical homogeneity of the phases present in the retrieved samples. Samples from experiments using this electrical cell did not present any chemical heterogeneity in the samples due to a significant thermal gradient across the sample (Pommier et al., 2015a,b; Zhang and Pommier, 2017).

We also computed the thermal gradient in the electrical cell using the CellAssembly numerical model for temperature distributions in cell assemblies developed by Hernlund et al. (2006). An example is presented in **Figure 7**. The sample considered for the calculations corresponds to a 1mm-long forsterite olivine disk and the electrodes are made of molybdenum. At 1200°C, the computed isotherms predict a small thermal gradient across the sample of 10°C or less, with the highest variations occurring laterally. The estimated current at this temperature is 187 A, which is in very good agreement with experimental values.

## IMPLICATIONS FOR THE EXPERIMENTAL COMMUNITY

The main motivation for developing this electrical cell for the 14/8 multi-anvil assembly is to make it available to the experimental community, in order to enhance cross-laboratory comparisons and thus, improve the quality of the electrical database for geoscience applications. The cell can be used to conduct both 2-electrode and 4-electrode electrical experiments, and has been tested with different types of materials (semi-conductors and conductors). The description of the cell parts used, their source and dimensions have been presented in order to make this technology available and facilitate the reproducibility of electrical experiments. We hope that the use of this electrical cell will promote technical discussions among the experimental community that will lead to improvements of the cell and new designs for future investigations. This electrical cell is available via COMPRES as a new cell assembly.

**Acknowledgments**

The authors acknowledge support from NSF-COMPRES IV EOID subaward. Use of the COMPRES Cell Assembly Project was also supported by COMPRES under NSF Cooperative Agreement EAR 1661511. AP thanks Jake Perez for technical help in the lab, Sabine Faulhaber (UCSD Nano-engineering Department) for technical assistance with SEM images, and Peter Asbeck and Jon Souders for discussions about the 4-electrode measurements. The thermal calculations used the freely available thermal modeling program CellAssembly (available at http://multianvil.asu.edu/Kurt's%20Thermal%20modelling/ThermalModeling.htm).

**REFERENCES**

Bauerle, J.E. (1969) Study of solid electrolyte polarization by a complex admittance method. Journal of Physics and Chemistry of Solids, 30: 2657-2670.

Constable, S. (2015) Geomagnetic induction studies. In Schuber–G. (Eds.), Treatise on Geophysics (Vol. 1, pp. 219–254). Amsterdam: Elsvier.

Deng, L., Seagle, C., Fei, Y., and Shahar, A. (2013) High pressure and temperature electrical resistivity of iron and implications for planetary cores. Geophysical Research Letters, 40, 33–37, doi:10.1029/2012GL054347.

Fogo, J.K., Benson, S.W., and Copeland, C.S. (1954) The electrical conductivity of supercritical solutions of sodium chloride and water. Journal of Chemical Physics, 22(2), 212- 216.

Glover, P. W. J., Hole, M. J., and Pous, J. (2000) A modified Archie's law for two conducting phases. Earth and Planetary Science Letters, 180 (3–4), 369–383, doi:10.1016/S0012-821X(00)00168-0.

Hernlund, J., Leinenweber, K., Locke, D., Tyburczy, J.A. (2006) A numerical model for steady-state temperature distributions in solid-medium high-pressure cell assemblies. American Mineralogist, 91 (2-3), 295–305.

Huebner, J. S., and Dillenburg, R. G. (1995) Impedance spectra of hot, dry silicate minerals and rock: qualitative interpretation of spectra. American Mineralogist, *80*(1-2), 46- 64.

Kavner, A., and D. Walker (2006) Core/mantle-like interactions in an electric field. Earth and Planetary Science Letters, 248, 316–329.

Kennedy, D.P. (1960) Spreading Resistance in Cylindrical Semiconductor Devices. Journal of Applied Physics, 31(8), 1490-1497.

Knight, R.J. (1984) The Dielectric Constant of Sandstones, 5Hz to 13MHz, Ph.D. dissertation, Stanford Univ., Stanford, Calif.

Koops, C.G. (1951) On the dispersion of resistivity and dielectric constant of some semiconductors at audio frequencies. Physical Review, 83(1), 121-124.

Kriaa, A., Hamdi, N., Jbali, K., Tzinmann, M. (2009) Corrosion of iron in highly acidic hydro-organic solutions. Corrosion Science 51, 668–676.

Lee, W.-J., Pyun, S.-I. (1999) Effects of hydroxide ion addition on anodic dissolution of pure aluminium in chloride ion-containing solution. Electrochimica Acta 44, 4041–4049.

Leinenweber, K., Tyburczy, J.A., Sharp, T.G., Soignard, E., Diedrich, T., Petuskey, W.B., Wang, Y., and Mosenfelder, J. (2012) Cell assemblies for reproducible multi-anvil experiments (the COMPRES assemblies). American Mineralogist, 97, 353-368.

Noyes et al. (1907) The electrical conductivity of aqueous solutions. Publication No63, Carnegie Institution of Washington, Washington, D.C.

Pommier A., F. Gaillard, M. Malki and M. Pichavant (2010) Methodological re-evaluation of the electrical conductivity of silicate melts. American Mineralogist, 95, 284–291.

Pommier A., K. Leinenweber, and M. Tasaka (2015a) Experimental Investigation of the Electrical Behavior of Olivine during Partial Melting under Pressure and Application to the Lunar Mantle. Earth and Planetary Science Letters, 425, 242–255.

Pommier A., K. Leinenweber, D. L. Kohlstedt, C. Qi, E. J. Garnero, S. Mackwell, J. Tyburczy (2015b) Experimental Constraints on the Electrical Anisotropy of the Lithosphere-Asthenosphere System. Nature, doi: 10.1038/nature14502.

Quist, A.V., and Marshall, W.L. (1968) Electrical conductances of aqueous sodium chloride solutions from 0 to 800°C and at pressures to 4000 bar. Journal of Physics and Chemistry, 72 2, p. 684.

Roberts, J.J. and Tyburczy, J.A. (1991) Frequency Dependent Electrical Properties of Polycrystalline Olivine Compact. Journal of Geophysical Research, 96, B10, 16,205-16,222.

Sato, H. (1986) High temperature a.c. electrical properties of olivine single crystal with varying oxygen partial pressure: Implications for the point defect chemistry. Physics of the Earth and Planetary Interiors, 41, 269-282.

Secco, R. A., and Schloessin, H. H. (1989) The electrical resistivity of solid and liquid Fe at pressures up to 7 GPa. Journal of Geophysical Research, 94, 5887–5894, doi:10.1029/JB094iB05p05887.

Silber, R.E., Secco, R.A., and Yong, W. (2017) Constant electrical resistivity of Ni along the melting boundary up to 9 GPa. Journal of Geophysical Research, 122, 5064–5081, doi:10.1002/2017JB014259.

Tyburczy, J. A., and D. K. Fisler (1995) Electrical properties of minerals and melts, in Mineral Physics and Crystallography: A Handbook of Physical Constants, Ref. Shelf, vol. 2, edited by T. J. Ahrens, pp. 185– 208, AGU, Washington, D. C.

Wang, D., Karato, S.-i., Jiang, Z. (2013) An experimental study of the influence of graphite on the electrical conductivity of olivine aggregates. Geophysical Research Letters 40, 2028–2032. http://dx.doi.org/10.1002/grl.50471.

Xu, Y., Poe, B.T., Shankland, T.J., Rubie, D.C. (1998) Electrical conductivity of olivine, wadsleyite and ringwoodite under upper-mantle conditions. Science 280, 1415–1418.

Yoshino, T., M.J. Walter, and T. Katsura (2003) Core formation in planetesimals triggered by permeable flow. Nature, 422, 154-157.

Yoshino, T., M.J. Walter, and T. Katsura (2004) Connectivity of molten Fe alloy in peridotite based on in situ electrical conductivity measurements: implications for core formation in terrestrial planets. Earth and Planetary Science Letters 222, 625-643.

Yoshino, T., E. Ito, T. Katsura, D. Yamazaki, S. Shan, X. Guo, M. Nishi, Y. Higo, and K. I. Funakoshi (2011) Effect of iron content on electrical conductivity of ferropericlase with implications for the spin transition pressure. Journal of Geophysical Research, 116, B04202, doi:10.1029/2010JB007801.

Zhang Z. and A. Pommier (2017) Electrical investigation of Metal-olivine systems and application to the core-mantle boundary for Mercury. Journal of Geophysical Research - Planets*,* 122. https://doi.org/10.1002/2017JE005390.

**FIGURE CAPTIONS**

**Figure 1**: Electrical cells developed for 2- and 4-electrode experiments using 14/8 COMPRES assemblies (A) and B), respectively). In both cases, W-Re wires are used as both thermocouples and electrodes.

**Figure 2**: Electrical cell design: Modifications from traditional 14/8 COMPRES assemblies to accommodate the electrode wires. A) 4-notch octahedron (pressure medium). B) 4-groove rhenium foil (furnace).

**Figure 3**: Effect of furnace chemistry on electrical measurements. Example of deformed polycrystalline San Carlos olivine at about 3 GPa (Pommier et al., under rev.) using graphite (black circles) or rhenium (empty circles) furnaces. No significant difference is observed on the electrical response, suggesting that the potential changes in the redox environment due to the furnace chemistry are negligible at the timescale of the experiments (about 2 hrs). The experiment performed with the rhenium furnace is more noisy because of issues due to the power supply that were unrelated to the cell assembly.

**Figure 4**: Examples of impedance spectra collected using the electrical cell (2-electrode measurements). X and Y axes correspond to the real and imaginary part of the complex impedance, respectively. Intersection of the sample's response with the real axis provides the value of the bulk electrical resistance. A) Hydrous olivine at 600°C and 4 GPa, from Pommier et al. (2015a). The semi-circle arc is typical of semiconductors. The presence of a second loop may indicate adsorption relaxation mechanisms (e.g., Lee and Pyun, 2009 and Kriaa et al., 2009) or chemical reactions (Wang et al., 2013) and its understanding requires further work. B) Two layer sample (one layer of San Carlos olivine, one layer of iron alloy,

with the volume ratio of olivine:metal being 0.7:1) at 400 and 975°C and 6 GPa (Zhang and Pommier, 2017). Here, the electrical response is dominated by the metal part of the sample. Spectra corrected from electrodes' contribution. C) Natural lawsonite at 500°C and 10 GPa (Pal et al., in prep.).

**Figure 5**: SEM images of retrieved samples after electrical experiments. A) EDS map on Fe-S alloy sample quenched at 4.4 GPa and 1470°C, showing the distribution of Mg, O, and Fe. The thin layer (<80 micron, in orange) at the interface between the metal sample and the MgO sleeve corresponds to ferropericlase. B) Back-scattered electron image of hydrous polycrystalline San Carlos olivine sample from Pommier et al. (2015a). Small electrode deformation is observed and should be accounted for as part of uncertainty calculations. Ferropericlase forms a layer (<100 micron thickness) at the interface between sample and MgO sleeve. The thin layer has a negligible contribution on the electrical measurements (see text for details).

**Figure 6**: Electrode contribution to the bulk electrical measurements using the 2-electrode configuration. The blank experiment was conducted at UCSD-SIO at about 3 GPa and at temperature up to about 1450C during heating (blue and green circles) and cooling (red circles) cycles. The constant value of about 7.5 ohms is similar to the one obtained at ASU using a comparable setup at 4 GPa (Pommier et al., 2015a).

**Figure 7**: Thermal profile in the electrical cell using the numerical model by Hernlund et al. (2006). Simulations are considering a forsterite sample at a temperature of 1200°C. Isotherms are indicated as black lines with the temperature interval between two isotherms being 100 °C. The temperature at the center of the assemblies is 1203°C; the temperature

DOI: https://doi.org/10.2138/am-2018-6448

at the contact between TC wire(s) and Mo electrode is 1200 °C and the temperature at the sample/MgO sleeve is 1211°C. The computed current is 187 A, which is in very good agreement with experiments at this temperature.

**Table 1. Components of the 14/8 electrical cell assembly (TC = thermocouple).**

| Material | Part | Source | Quantity for one experiment | Density[a] (g/mL) | Porosity[a] (%) |
|---|---|---|---|---|---|
| MgO-spinel (MG-ASU) | Octahedron | Ceramco | 1 | 2.97 | 16.70 |
| Zirconia | Inner sleeve | Mino Yogyo OZ-8C-HD | 1 | 3.80 | 28.80 |
| Rhenium, 63 micron foil | Furnace | Rhenium Alloys | 1 | 21.02 | 0.00 |
| MgO | 4-bore (TC) | Saint-Gobain | 2 | 2.41 | 32.60 |
| MgO | Sample sleeve | Saint-Gobain | 1 | 2.41 | 32.60 |
| MgO | TC sleeve | Saint-Gobain | 2 | 2.41 | 32.60 |
| Mo | Electrode (disk or square) | Alfa | 2 | 10.22 | 0.00 |
| Fe | Electrode (disk or square) | Goodfellow | 2 | 7.87 | 0.00 |
| W-Re | TC wire (C-type) | Concept Alloys | 3 or 4[b] | - | - |
| Mullite | TC insulation sleeve | Coors | 6 or 8[b] | 2.10 | >30 |
| Ceramic adhesive | Part # 919 | Cotronics | - | - | - |
| Paper, 3-ply | Sheet around WC cubes | Anchor paper | 4 | - | - |
| Pyrophylite | Gaskets around WC cubes | Bar-Io | 12[c] | 2.69 | 4.30 |

[a] From Leinenweber et al. (2012)

[b] The number depends on the type of electrical measurements (2 or 4-electrode experiments)

[c] Two sizes ("long" and "short"). See Leinenweber et al. (2012) for details.

DOI: https://doi.org/10.2138/am-2018-6448

# Figure 1

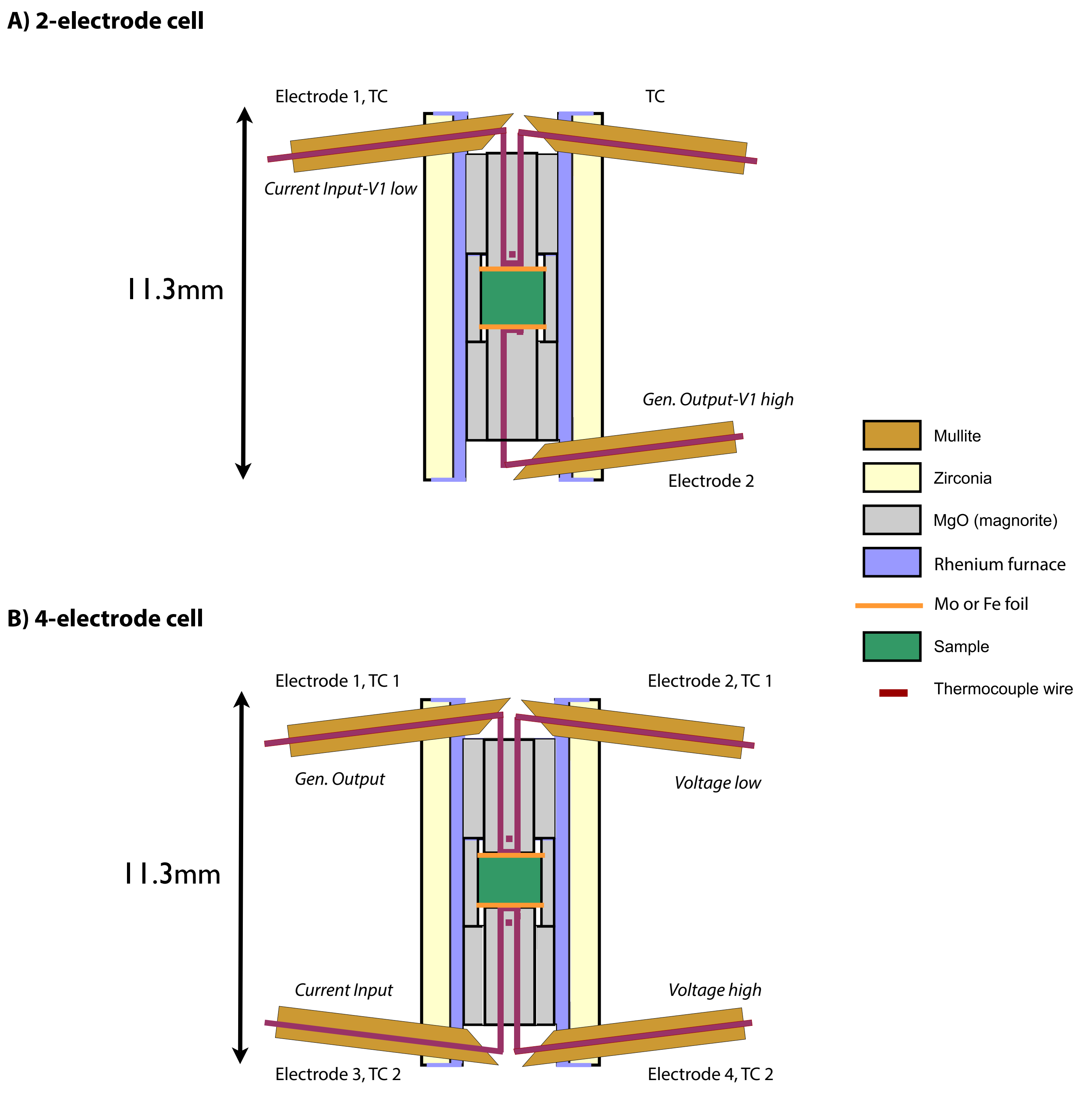

**Figure 2**

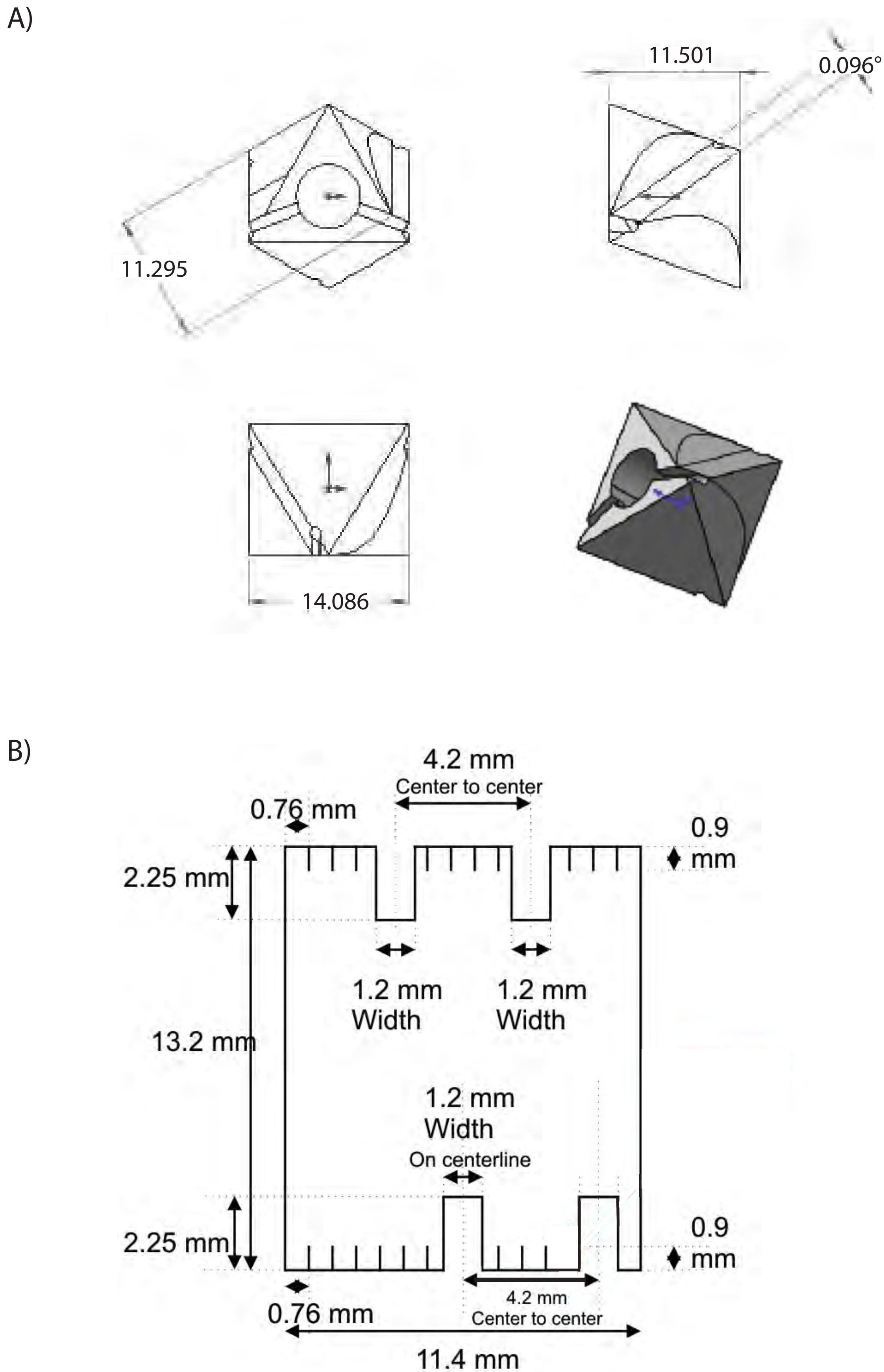
A)
11.501
0.096°
11.295
14.086
B)
4.2 mm
Center to center
0.76 mm
0.9
mm
2.25 mm
1.2 mm
Width
1.2 mm
Width
13.2 mm
1.2 mm
Width
On centerline
2.25 mm
0.9
mm
0.76 mm
4.2 mm
Center to center
11.4 mm

DOI: https://doi.org/10.2138/am-2018-6448

**Figure 3**

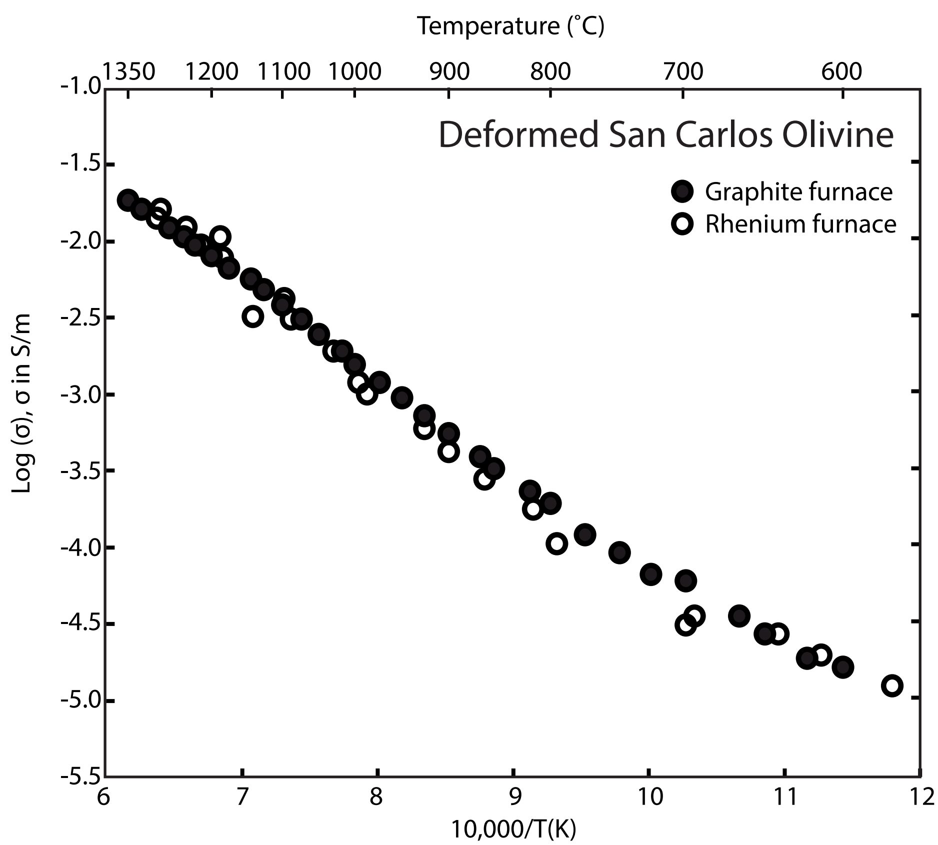

# Figure 4

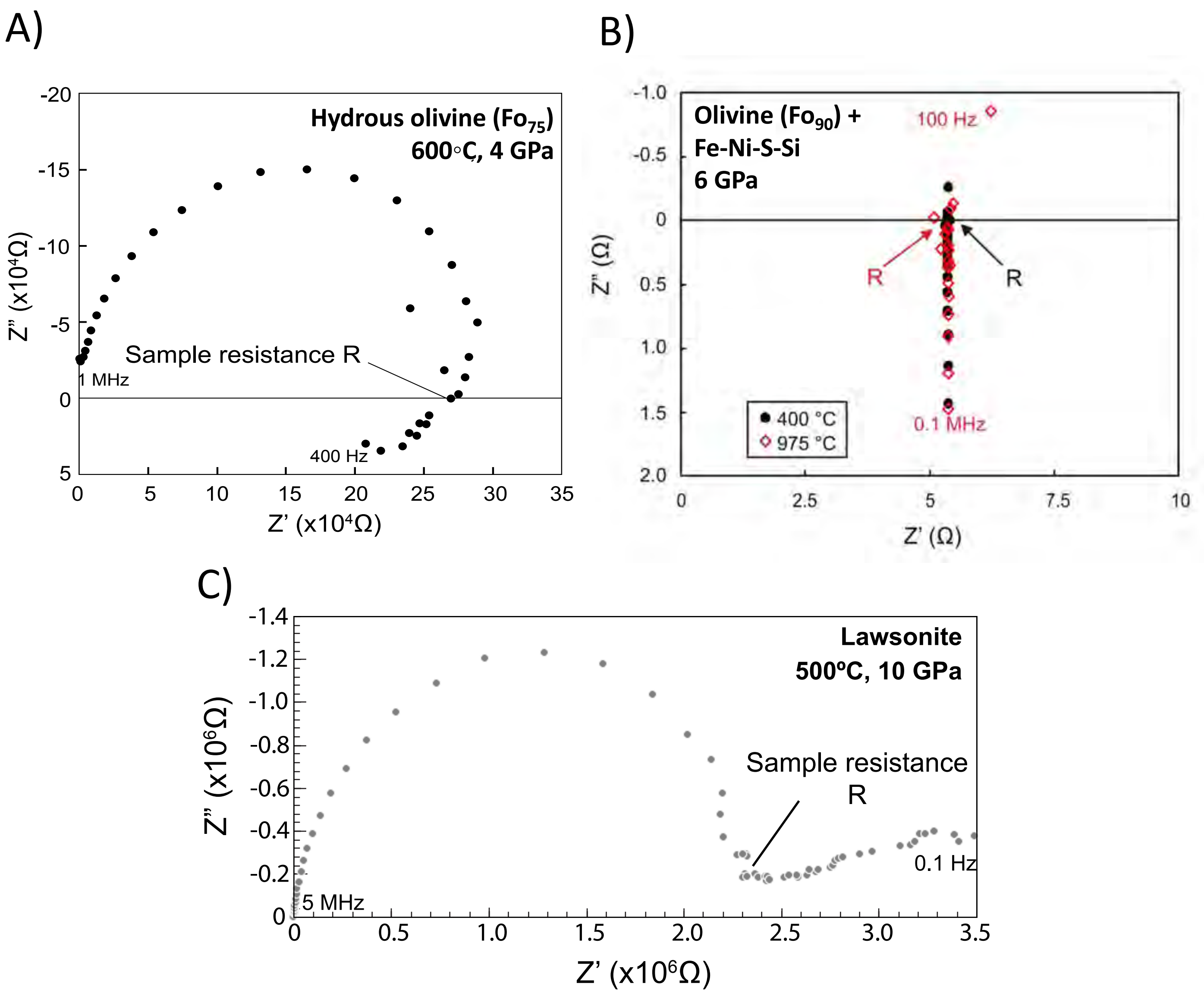
A)
Hydrous olivine ($Fo_{75}$)
600◦C, 4 GPa
Sample resistance R
1 MHz
400 Hz
Z" (x10⁴Ω)
Z' (x10⁴Ω)
B)
Olivine ($Fo_{90}$) +
Fe-Ni-S-Si
6 GPa
100 Hz
0.1 MHz
R
R
400 °C
975 °C
Z" (Ω)
Z' (Ω)
C)
Lawsonite
500ºC, 10 GPa
Sample resistance
R
5 MHz
0.1 Hz
Z" (x10⁶Ω)
Z' (x10⁶Ω)

This is a preprint, the final version is subject to change, of the American Mineralogist (MSA)
Cite as Authors (Year) Title. American Mineralogist, in press.
DOI: https://doi.org/10.2138/am-2018-6448

Figure 5

A)

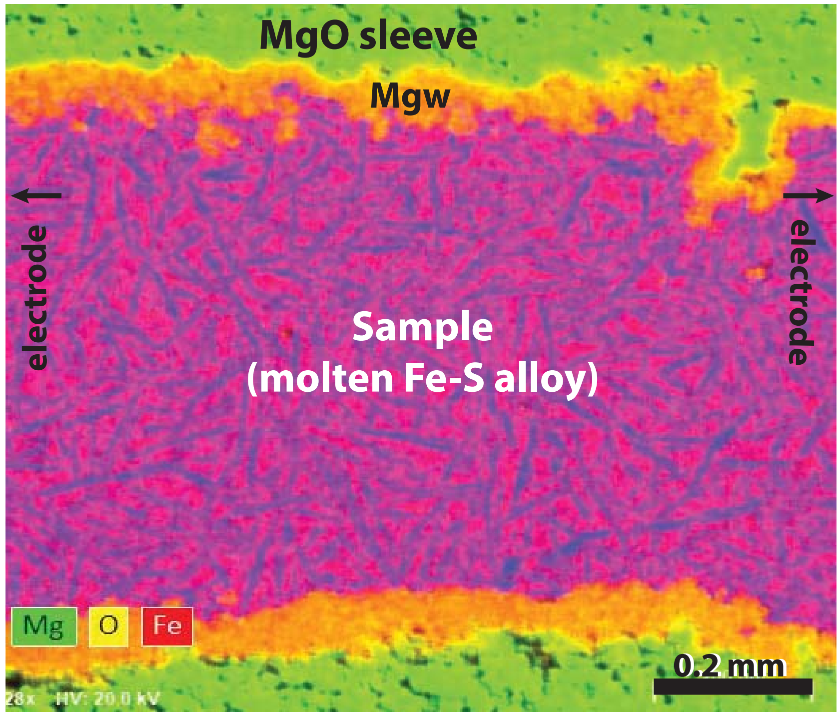


B)

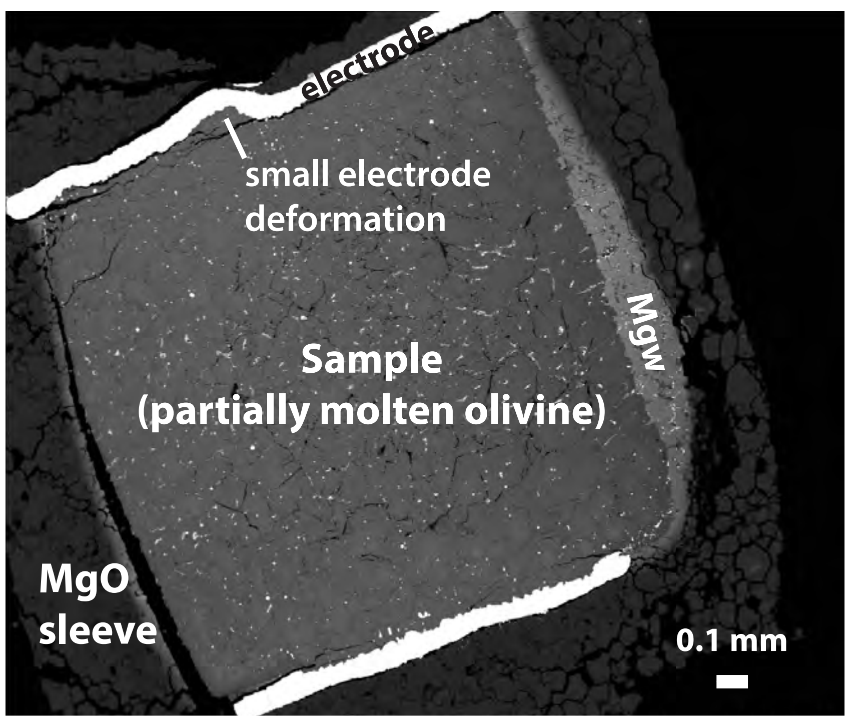

DOI: https://doi.org/10.2138/am-2018-6448

# Figure 6

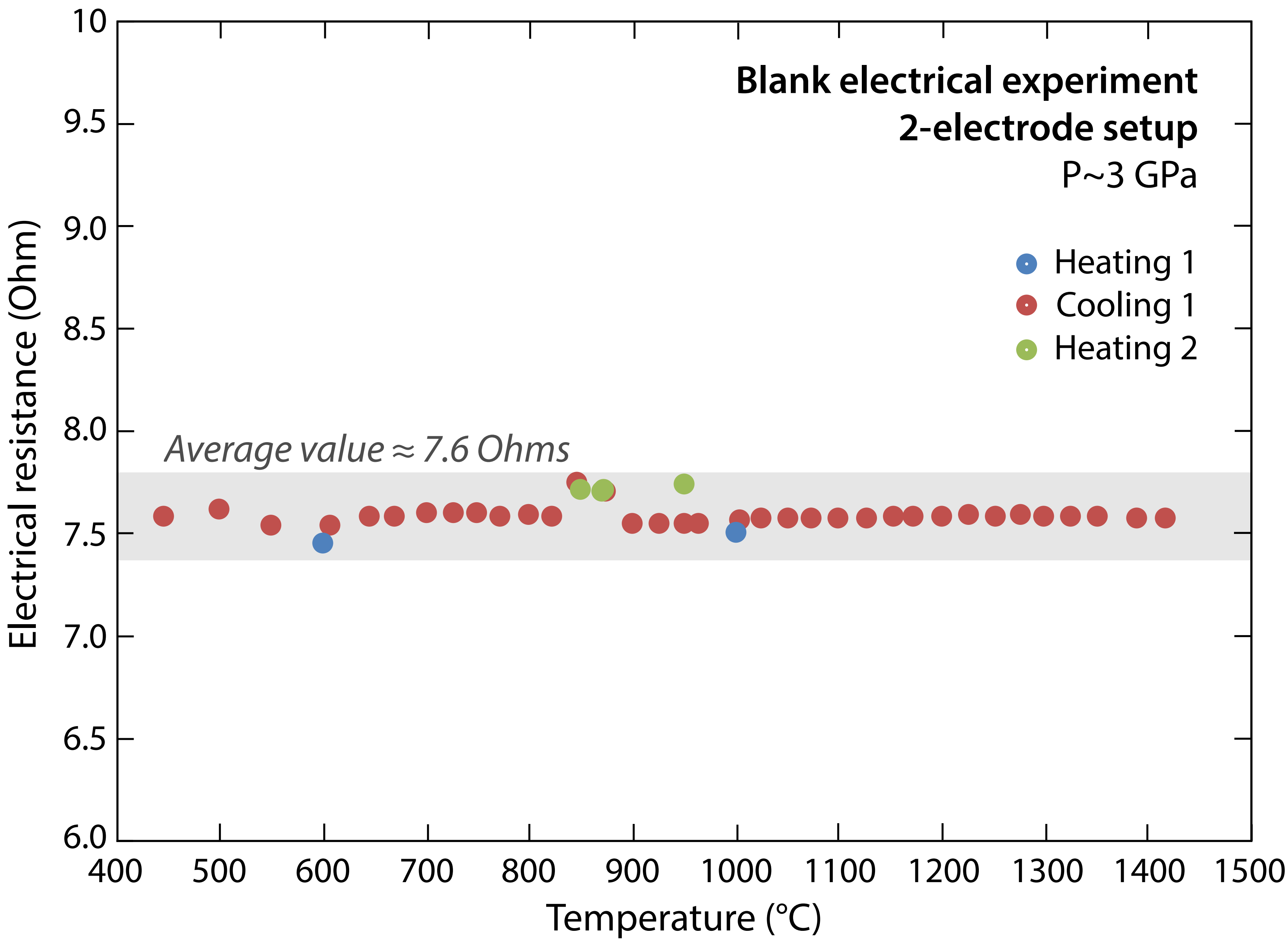

This is a preprint, the final version is subject to change, of the American Mineralogist (MSA)
Cite as Authors (Year) Title. American Mineralogist, in press.
DOI: https://doi.org/10.2138/am-2018-6448

**Figure 7**